PTEP

Prog. Theor. Exp. Phys. **2024** 033B01 (22 pages)
DOI: 10.1093/ptep/ptae016

# Casimir Effect of Lorentz-Violating Charged Dirac Field in Background Magnetic Field

Ar Rohim [1,2,*], Arista Romadani [3], and Apriadi Salim Adam [1]

[1] *Research Center for Quantum Physics, National Research and Innovation Agency (BRIN), South Tangerang 15314, Indonesia*
[2] *Departemen Fisika, Fakultas Matematika dan Ilmu Pengetahuan Alam (FMIPA), Universitas Indonesia, Depok 16424, Indonesia*
[3] *Department of Physics, Faculty of Science and Technology, Universitas Islam Negeri Maulana Malik Ibrahim Malang, Malang 65144, Indonesia*
*Email: ar.rohim@ui.ac.id

Received August 29, 2023; Revised January 24, 2024; Accepted January 25, 2024; Published January 27, 2024

We study the effect of the Lorentz violation on the Casimir energy and pressure of a charged Dirac field in a background uniform magnetic field. In the model, the Lorentz violation is parameterized not only by the intensity but also by its direction. We investigate two cases of the direction of violation, namely, time-like and space-like vector cases. We use the boundary condition of the MIT bag model to represent the property of the plates. We show how the Lorentz violation and the magnetic field affect the structure of the Casimir energy and its pressure. We also investigate the weak and strong magnetic field cases with two different limits, heavy and light masses. In addition, we compute the ratio of the influence of the strong magnetic field to that of the weak one for the Casimir energy and its pressure. We find that the strong magnetic field enhances the magnitude of the Casimir energy and its pressure, where the parameter of the intensity of Lorentz violation could scale the plate's distance.

Subject Index A64, B30, B69

## 1. Introduction

The Casimir effect representing quantum field effects under macroscopic boundaries was first predicted by H. B. G. Casimir in 1948 [1]. He showed that the quantum vacuum fluctuations of the electromagnetic field confined between two parallel plates generate an attractive force. One decade later, in 1958, Sparnaay performed the experimental measurement of the effect; however, with only rough precision [2]. He found that the attractive force of the plates does not contradict the theoretical prediction. After his work, studies have shown the Casimir effect to be experimentally confirmed with high precision [3–6]. The Casimir effect itself has many applications in nanotechnology [7], and the theoretical discussion was elaborated in connection to several research areas, e.g. cosmology [8] and condensed matter physics [9,10] (see e.g. Refs. [11,12] for reviews).

The studies showed that the Casimir effect also arises not only for the electromagnetic field but also for other fields. The geometry of the plate's surface represented by the form of the boundary conditions also determines how the Casimir effect behaves. To discuss the Casimir effect of the scalar field, one can use the Dirichlet boundary conditions of the vanishing field at the surface of the plates. In such a case, one can also employ Neumann and/or mixed boundary


Funded by SCOAP[3]

conditions [13]. However, in the case of the fermion field, one cannot apply such boundaries because the solution for the fermion field is derived from the first-order differential equation. Alternatively, one may use a bag boundary condition that guarantees the flux vanishing at the plate's surface. The well-known form covering this property is the boundary condition from the MIT bag model [14,15] (see Ref. [16] for a review). The extension of this boundary that includes the role of the chiral angle has been employed in the literature (see, e.g. Refs. [17,18], cf. Ref. [19] for the self-adjoint variant).

The Casimir effect phenomenon could be investigated in the system with charged quantum fields under the magnetic field background. With such a system, one can investigate how the charged quantum field couples to the quantum fluctuation [19–25]. On the other hand, the Casimir effect in the system involving a Lorentz violation has also attracted some attention [26–33] (see also Refs. [34,35] for another approach under the Horava–Lifshitz theories [36]). Within the framework of string theories, spontaneous Lorentz breaking may occur through a dynamic of the Lorentz covariant [37]. Such a dynamic will generate interactions to gain nonzero expectation values for Lorentz tensors. This is the same analog as in the Higgs mechanism in the context of the standard model. Several studies have investigated a system under Lorentz symmetry breaking and the CPT anomaly [38–40]. These violations could possibly be measured in the proposed experiment, e.g. the measurements of neutral-meson oscillations [41–47], the quantum electrodynamics test on Penning traps [48–53], and the baryogenesis mechanism [54] (see Ref. [55] for the experimental data of Lorentz and CPT violations). Hence, in this work, we study a system of charged fields involving both Lorentz violation and a magnetic field background. In particular, we investigate the Casimir effect of the system under such effects.

In our setup, the magnetic field is raised in parallel to the normal plate's surface. We investigate two cases of the Lorentz-violating direction, i.e. time-like and space-like directions. For the space-like case, we restrict ourselves to discussing the violation in the $z$-direction only because Lorentz violation in the $x$- and $y$-directions does not affect the behavior of the Casimir energy of a Dirac field [28]. In the present study, we employ the boundary condition from the MIT bag model [14–16], which was originally used to describe quark confinement. It is natural to show that the presence of the boundary condition in the confinement system leads the allowed perpendicular momentum to the boundary surface to be discrete. To discuss the Casimir effect, we investigate the mode expansion of the field consisting of the linear superposition of the positive- and negative-energy solutions associated with the creation and annihilation operators. We can evaluate the vacuum energy by applying the boundary condition to the mode expansion. In the present study, we use the Abel–Plana-like summation [56] to extract the divergence of the vacuum energy in the presence of boundary conditions. Then, the Casimir energy can be mathematically obtained by taking the difference between the vacuum energy in the presence of the boundary conditions and that in their absence, where both vacuum energies are infinite, but their difference is finite.

The structure of the rest of this paper is organized as follows. In Sect. 2, we describe the model of our system, namely, a Dirac field confined between two parallel plates with a background magnetic field under the Lorentz violation in the quantum field theory framework. In Sect. 3, we investigate the Casimir energy. In this section, we derive the solution for the field inside the confinement area following the procedure used in the literature (see, e.g. Refs. [19,57,58]). In Sect. 4, we discuss the Casimir pressure. Section 5 is devoted to our summary. In this paper, we use natural units so that $c = \hbar = 1$.

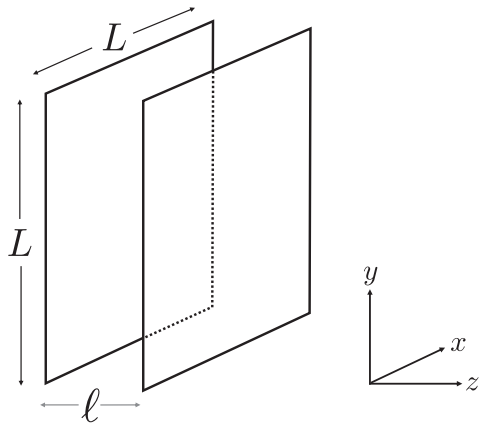


**Fig. 1.** Physical setup: Dirac field confined between two parallel plates separated by the distance $\ell$. The plates with the surface area $L^2$ are placed at the $xy$-plane. In this work, we assume the limit $L \to \infty$ approximately.

## 2. Model

We consider the charged Dirac field confined between two parallel plates placed at $z = 0$ and $z = \ell$ in the presence of a uniform magnetic field. The normal surface of the plates is parallel to the $z$-axis (see Fig. 1).

In our model, the Lorentz symmetry is not preserved. Models with the spirit of Lorentz violation have been proposed in Refs. [28,33,59–64]. The Lagrangian density of a Dirac field with mass $m$ for such a system is given by

$$\mathcal{L} = \bar{\Psi}\big[i\gamma^\mu\partial_\mu - e\gamma^\mu A_\mu - m + i\lambda u^\mu u^\nu\gamma_\mu\partial_\nu\big]\Psi, \tag{1}$$

where $\bar{\Psi}(\equiv \Psi\gamma^0)$ is the Dirac adjoint, $\lambda$ is the dimensionless parameter with $|\lambda| \ll 1$, $A_\mu$ is the four vector potential, and $u^\mu$ is an arbitrary constants vector where $u^\mu u_\mu$ can be 1, $-1$, 0 for time-like, space-like, and light-like, respectively. The Lorentz symmetry breaking is characterized by the last term of Eq. (1); the parameter $\lambda$ contributes to the violation intensity whereas the vector $u^\mu$ describes the violation direction [33]. In the present study, we use $4 \times 4$ gamma matrices $\gamma^\mu$ written in the Dirac representation as follows:

$$\gamma^0 = \begin{pmatrix} I & 0 \\ 0 & -I \end{pmatrix} \quad \text{and} \quad \gamma^j = \begin{pmatrix} 0 & \sigma^j \\ -\sigma^j & 0 \end{pmatrix}, \quad j = 1, 2, 3, \tag{2}$$

where $I$ represents the $2 \times 2$ identity matrix and $\sigma^j$ is the $2 \times 2$ Pauli matrices. The gamma matrices satisfy the anticommutation relation as $\{\gamma^\mu, \gamma^\nu\} = \eta^{\mu\nu}$, where $\eta^{\mu\nu}(\equiv \text{diag.}(1, -1, -1, -1))$ is the metric tensor of the Minkowski spacetime.

The Dirac field $\Psi$ satisfies the modified Dirac equation as follows:

$$[i\gamma^\mu\partial_\mu - e\gamma^\mu A_\mu - m + i\lambda u^\mu u^\nu\gamma_\mu\partial_\nu]\Psi = 0. \tag{3}$$

The positive-energy solution for the above Dirac equation is given as

$$\Psi^{(+)}(r) = e^{-i\omega t}\psi(\boldsymbol{r}) = e^{-i\omega t}\begin{pmatrix} \chi_1 \\ \chi_2 \end{pmatrix}, \tag{4}$$

where $\chi_1$ and $\chi_2$ are the upper and lower two-component spinors, respectively. We use $\omega$ to represent the eigenenergy of the Dirac field. In our model, the magnetic field is raised in the $z$-direction $\boldsymbol{B} = (0, 0, B)$, where one can choose the corresponding four-vector potential com-

ponents as follows:

$$A_0 = A_2 = A_3 = 0 \quad \text{and} \quad A_1 = -yB, \tag{5}$$

with $B$ as the magnetic field strength.

The geometry of the plates is described by the boundary condition from the MIT bag model as follows [14–16]:

$$in_\mu \gamma^\mu \Psi = \Psi, \tag{6}$$

where $n_\mu$ is the unit normal inward four-vector perpendicular to the boundary surface. The consequence of this boundary is the vanishing flux or normal probability density at the plate surface $n_\mu J^\mu (\equiv n_\mu \bar{\Psi} \gamma^\mu \Psi) = 0$. The idea of this boundary is that the mass of the field is written as a function of its position; inside the confinement area, the mass has a finite value and becomes infinite at the boundary surface. Then, one can suppose that the field outside the confinement area vanishes (see Ref. [65] for the confinement model of a relativistic particle). While inside the confinement area, the solution for the field is written as the superposition between the left- and right-field components.

## 3. Casimir energy

In this section, we derive the Casimir energy of a Lorentz-violating charged Dirac field in a background magnetic field. We study two directions of the Lorentz violation, namely, time-like and space-like vector cases. We do not consider the light-like case because the contribution from the Lorentz violation term will vanish and the result of the Casimir energy is the same as in Ref. [19]. We derive the solution for the Dirac field inside the confinement area under the boundary condition from the MIT bag model [14–16]. We follow the general procedure given in Refs. [19,57,58]. Then, we compute the Casimir energy using the Abel–Plana-like summation [56] following Refs. [17,33,66]. In addition, we also investigate the Casimir energy approximately for the case of weak and strong magnetic fields.

### 3.1. *Time-like vector case*

We consider the positive-energy solution for the time-like vector case with $u^{(t)} = (1, 0, 0, 0)$. In this case, the Dirac Eq. (3) gives two equations as follows:

$$[(1+\lambda)\omega - m]\chi_1^{(t)} = (-i\sigma^j \partial_j + eyB\sigma^1)\chi_2^{(t)}, \tag{7}$$

$$[(1+\lambda)\omega + m]\chi_2^{(t)} = (-i\sigma^j \partial_j + eyB\sigma^1)\chi_1^{(t)}, \tag{8}$$

from which we have the equation for the upper two-component spinor $\chi_1^{(t)}$ as

$$\begin{aligned}[(1+\lambda)^2\omega^2 - m^2]\chi_1^{(t)} &= (-i\sigma^j \partial_j + eyB\sigma^1)^2 \chi_1^{(t)} \\ &= [-\nabla^2 + e^2y^2B^2 - eB(i2y\partial_1 + \sigma^3)]\chi_1^{(t)}.\end{aligned} \tag{9}$$

In the above equation, we have used the commutation and anticommutation relations of the Pauli matrices given as $[\sigma^l, \sigma^m] = 2i\epsilon_{lmn}\sigma^n$ and $\{\sigma^m, \sigma^n\} = 2\delta_{mn}I$, respectively, where $\delta_{mn}$ is a Kronecker delta and $\epsilon_{lmn}$ is a Levi-Civita symbol. To find the solution for $\chi_1^{(t)}$ in Eq. (9), one can propose the following form:

$$\chi_1^{(t)} = e^{ik_1 x} e^{ik_3 z} \mathrm{F}^{(t)}(y). \tag{10}$$

The presence of the Pauli matrix $\sigma^3$ in Eq. (9) leads to two independent solutions for $\mathrm{F}^{(t)}(y)$ as follows:

$$\mathrm{F}_{+}^{(t)}(y) = \begin{pmatrix} \mathrm{f}_{+}^{(t)}(y) \\ 0 \end{pmatrix} \quad \text{and} \quad \mathrm{F}_{-}^{(t)}(y) = \begin{pmatrix} 0 \\ \mathrm{f}_{-}^{(t)}(y) \end{pmatrix}. \tag{11}$$

Then, it is convenient to introduce $s = \pm 1$ so that the solution for $\mathrm{f}_{s}^{(t)}(y)$ can be read in a general way as

$$\sigma^3 \mathrm{F}_{s}^{(t)}(y) = s\mathrm{F}_{s}^{(t)}(y), \tag{12}$$

and introduce a new parameter as

$$\xi^{(+,t)} = \sqrt{eB}\big(y + \frac{k_1}{eB}\big). \tag{13}$$

Then, Eq. (9) can be read as Hermite's equation for arbitrary $s$ as follows:

$$\left[\frac{d^2}{d\xi^{(t)2}} - \xi^{(t)2} + a_s^{(t)}\right]\mathrm{f}_{s}^{(t)}(y) = 0, \tag{14}$$

where

$$a_s^{(t)} = \frac{(1+\lambda)^2\omega^2 - m^2 - k_3^2 + eBs}{eB}. \tag{15}$$

We now have the eigenenergies as[1]

$$\omega_{n',k_3}^{(t)} = (1+\lambda)^{-1}\sqrt{m^2 + k_3^2 + |eB|(2n'+1) - |eB|s}, \tag{16}$$

where we have used $a_s^{(t)} = 2n' + 1$ with $n' = 0, 1, 2, 3, \cdots$. The appropriate solution for $\mathrm{f}_{s}^{(t)}(y)$ with positive value $eB$ that satisfies Hermite's Eq. (14) is given by

$$\mathrm{f}_{s}^{(t)}(y) = \sqrt{\frac{(eB)^{1/2}}{2^n n'!(\pi)^{1/2}}} e^{-\xi^2/2} H_{n'}(\xi^{(t)}), \tag{17}$$

where $\mathrm{f}_{s}^{(t)}(y)$ has been normalized. The solution for $\mathrm{F}_{s}^{(t)}(y)$ is characterized by two conditions, namely, $n' = n$ for $s = +1$ and $n' = n - 1$ for $s = -1$. They can be written as follows:

$$\mathrm{F}_{+}^{(t)}(y) = \begin{pmatrix} \mathrm{f}_{k_1,n}^{(t)}(y) \\ 0 \end{pmatrix} \quad \text{and} \quad \mathrm{F}_{-}^{(t)}(y) = \begin{pmatrix} 0 \\ \mathrm{f}_{k_1,n-1}^{(t)}(y) \end{pmatrix}. \tag{18}$$

We note that the eigenenergy for both values of $s$ gives the same expression as

$$\omega_{n,k_3}^{(t)} = (1+\lambda)^{-1}\sqrt{m^2 + k_3^2 + 2n|eB|}, \tag{19}$$

where $n = 0, 1, 2, 3, \cdots$ is the Landau level. Then, we can finally derive the spatial solution for the right-moving field component as follows:

$$\begin{aligned}\psi_{k_1,n,k_3}^{(+,t)}(\boldsymbol{r}) = {} & \frac{e^{ik_1x}e^{ik_3z}}{2\pi\sqrt{2(1+\lambda)\omega_{n,k_3}^{(t)}((1+\lambda)\omega_{n,k_3}^{(t)} + m)}} \\ & \times \left[C_1 \begin{pmatrix} ((1+\lambda)\omega_{n,k_3}^{(t)} + m)\mathrm{f}_{k_1,n}^{(t)}(y) \\ 0 \\ k_3\mathrm{f}_{k_1,n}^{(t)}(y) \\ \sqrt{2neB}\mathrm{f}_{k_1,n-1}^{(t)}(y) \end{pmatrix} + C_2 \begin{pmatrix} 0 \\ ((1+\lambda)\omega_{n,k_3}^{(t)} + m)\mathrm{f}_{k_1,n-1}^{(t)}(y) \\ \sqrt{2neB}\mathrm{f}_{k_1,n}^{(t)}(y) \\ -k_3\mathrm{f}_{k_1,n-1}^{(t)}(y) \end{pmatrix}\right],\end{aligned} \tag{20}$$

[1] We have used $|eB|$ to avoid imaginary values of $\omega$.

and

$$\psi^{(+,t)}_{k_1,0,k_3}(\boldsymbol{r}) = \frac{e^{ik_1x}e^{ik_3z}}{2\pi\sqrt{2(1+\lambda)\omega^{(t)}_{0,k_3}((1+\lambda)\omega^{(t)}_{0,k_3}+m)}} C_0 \mathrm{f}^{(t)}_{k_1,0}(y) \begin{pmatrix} (1+\lambda)\omega^{(t)}_{0,k_3}+m \\ 0 \\ k_3 \\ 0 \end{pmatrix}, \tag{21}$$

for $n \geq 0$ and $n = 0$, respectively, where $C_0$, $C_1$, and $C_2$ represent the complex coefficients and $\mathrm{f}^{(t)}_{k_1,n}(y)$ is given by

$$\mathrm{f}^{(t)}_{k_1,n}(y) = \sqrt{\frac{(eB)^{1/2}}{2^n n!\pi^{1/2}}} \exp\left[-\frac{eB}{2}\left(y+\frac{k_1}{eB}\right)^2\right] H_n\left[\sqrt{eB}\left(y+\frac{k_1}{eB}\right)\right], \tag{22}$$

with $H_n(\xi)$ as the Hermite polynomial. In a similar way, we can obtain the solution for the left-moving field component as follows:

$$\begin{aligned}\psi^{(+,t)}_{k_1,n,-k_3}(\boldsymbol{r}) = {} & \frac{e^{ik_1x}e^{-ik_3z}}{2\pi\sqrt{2(1+\lambda)\omega^{(t)}_{n,k_3}((1+\lambda)\omega^{(t)}_{n,k_3}+m)}} \\ & \times \left[\tilde{C}_1 \begin{pmatrix} ((1+\lambda)\omega_{nk_3}+m)\mathrm{f}^{(t)}_{k_1,n}(y) \\ 0 \\ -k_3\mathrm{f}^{(t)}_{k_1,n}(y) \\ \sqrt{2neB}\mathrm{f}^{(t)}_{k_1,n-1}(y) \end{pmatrix} + \tilde{C}_2 \begin{pmatrix} 0 \\ ((1+\lambda)\omega_{nk_3}+m)\mathrm{f}^{(t)}_{k_1,n-1}(y) \\ \sqrt{2neB}\mathrm{f}^{(t)}_{k_1,n}(y) \\ k_3\mathrm{f}^{(t)}_{k_1,n-1}(y) \end{pmatrix}\right],\end{aligned} \tag{23}$$

and

$$\psi^{(+,t)}_{k_1,0,-k_3}(\boldsymbol{r}) = \frac{e^{ik_1x}e^{-ik_3z}}{2\pi\sqrt{2(1+\lambda)\omega^{(t)}_{0,k_3}((1+\lambda)\omega^{(t)}_{0,k_3}+m)}} \tilde{C}_0 \mathrm{f}^{(t)}_{k_1,0}(y) \begin{pmatrix} (1+\lambda)\omega^{(t)}_{0,k_3}+m \\ 0 \\ -k_3 \\ 0 \end{pmatrix}, \tag{24}$$

for $n \geq 1$ and $n = 0$, respectively, where $\tilde{C}_0$, $\tilde{C}_1$, and $\tilde{C}_2$ are the complex coefficients. The total field solution is given by the linear combination of the left- and right-moving field components as follows:[2]

$$\psi^{(+,t)}_{k_1,n,k_3}(\boldsymbol{r}) = \psi^{(+,t)}_{k_1,n,k_3}(\boldsymbol{r}) + \psi^{(+,t)}_{k_1,n,-k_3}(\boldsymbol{r}), \tag{25}$$

where we use $k_{3l}$ to represent the allowed momentum in the system, as we will see below.

For arbitrary nonzero complex coefficients, we have the constraint for the momentum component in the $z$-direction ($k_3$) in the case of $n \geq 0$ as follows:

$$m\ell \sin(k_3\ell) + k_3\ell\cos(k_3\ell) = 0. \tag{26}$$

The detailed derivation is given in Appendix A. The solution for Eq. (26) is given by $k_{3l}$ with $l = 1, 2, 3, \cdots$, which indicates that the allowed momentum $k_3$ must be discrete. As a consequence, the energy of the field under the MIT boundary condition must also be discrete as follows:

$$\omega^{(t)}_{n,l} = (1+\lambda)^{-1}\sqrt{m^2 + k^2_{3l} + 2n|eB|}. \tag{27}$$

These properties not only hold for positive-energy solutions but also for the negative-energy counterparts. One can see that the magnetic field and parameter $\lambda$ do not affect the structure of the momentum constraint (26).

[2]In the case of preserved Lorentz symmetry ($\lambda = 0$), the solution is completely the same as that of Ref. [19].

We now write down a mode expansion of the Dirac field in the time-like vector case under the boundary condition from the MIT bag model as

$$\Psi^{(t)}_{k_1,n,l}(r) = \sum_{n=0}^{\infty}\sum_{l=1}^{\infty}\int_{-\infty}^{\infty} dk_1\big[\hat{a}_{k_1,n,l}\Psi^{(+,t)}_{k_1,n,l}(r) + \hat{b}^{\dagger}_{k_1,n,l}\Psi^{(-,t)}_{k_1,n,l}(r)\big], \tag{28}$$

where $\Psi^{(\pm,t)}_{k_1,n,l}(r)$ are the positive $(+)$ and negative $(-)$ energy solutions. See Appendix B.1 for the detailed expression of the negative-energy solution. The annihilation and creation operators in Eq. (28) satisfy the following anticommutation relations:

$$\{\hat{a}_{k_1,n,l}, \hat{a}^{\dagger}_{k_1',n',l'}\} = \{\hat{b}_{k_1,n,l}, \hat{b}^{\dagger}_{k_1',n',l'}\} = \delta_{nn'}\delta_{ll'}\delta(k_1 - k_1'), \tag{29}$$

and the other anticommutation relations vanish. The Dirac field satisfies orthonormality conditions as follows:

$$\int d\boldsymbol{x}_{\perp}\int_0^{\ell} dz\psi^{(j,t)\dagger}_{k_1,n,l}(\boldsymbol{r})\psi^{(j',t)}_{k_1',n',l'}(\boldsymbol{r}) = \delta_{jj'}\delta_{nn'}\delta_{ll'}\delta(k_1 - k_1'), \quad j, j' = 0, 1, 2\,, \tag{30}$$

by which we can obtain the relations of the complex coefficients of the field. We use $\boldsymbol{x}_{\perp} \equiv (x, y)$ to represent the subspatial coordinate parallel to the normal plates' surface. From the above Lagrangian density (1), one can obtain the Hamiltonian density in the time-like vector case as follows:

$$\mathcal{H}^{(t)} = -\bar{\Psi}^{(t)}\big[i\gamma^j\partial_j - e\gamma^{\mu}A_{\mu} - m\big]\Psi^{(t)} = i(1+\lambda)\Psi^{(t)\dagger}\partial_0\Psi^{(t)}. \tag{31}$$

Now we are ready to evaluate the vacuum energy as follows:

$$E^{(t)}_{\text{Vac.}} = \int_{\Omega} d^3\boldsymbol{x}\mathcal{E}^{(t)}_{\text{Vac.}} = \int_{\Omega} d^3\boldsymbol{x}\langle 0|\mathcal{H}^{(t)}|0\rangle = -\frac{|eB|L^2}{\pi}\sum_{n=0}^{\infty}\sum_{l=1}^{\infty} i_n\sqrt{m^2 + \left(\frac{k_{3l}'}{\ell}\right)^2 + 2n|eB|}, \tag{32}$$

where $\mathcal{E}_{\text{Vac.}}$ is the vacuum energy density, $i_n = 1 - \frac{1}{2}\delta_{n0}$, $k_{3l}' \equiv k_{3l}\ell$, and $\Omega$ is the volume of the confinement area. One can derive the Casimir energy by subtracting the vacuum energy in the presence of the boundary condition from that in the absence of one. We note that the roles of $\lambda$ do not appear in the vacuum energy for the time-like vector case. In other words, the Casimir energy also does not depend on $\lambda$. In the next subsection, we will show that the above result can be recovered in the case of preserved Lorentz symmetry. Therefore, it is not necessary to evaluate further the Casimir energy in this subsection.

### 3.2. *Space-like vector case*

In this subsection, we investigate the Casimir energy for the space-like vector case in the $z$-direction. We start the discussion by deriving the positive energy solution for the space-like vector case with $u^{(z)} = (0, 0, 0, 1)$. In this case, the Dirac Eq. (3) gives two equations as follows:

$$(\omega - m)\chi_1^{(z)} = (-i\sigma^j\partial_j + eyB\sigma^1 + i\lambda\sigma^3\partial_3)\chi_2^{(z)}, \tag{33}$$

$$(\omega + m)\chi_2^{(z)} = (-i\sigma^j\partial_j + eyB\sigma^1 + i\lambda\sigma^3\partial_3)\chi_1^{(z)}. \tag{34}$$

Multiplying both sides of Eq. (33) by $(\omega + m)$ and using Eq. (34), we have the equation for the upper two-component spinor $\chi_1^{(z)}$ as follows:

$$\begin{aligned}(\omega^2 - m^2)\chi_1^{(z)} &= (-i\sigma^j\partial_j + eyB\sigma^1 + i\lambda\sigma^3\partial_3)^2\chi_1^{(z)} \\ &= [-\nabla^2 + e^2y^2B^2 - eB(2iy\partial_1 + \sigma^3) + 2\lambda\partial_3^2 - \lambda^2\partial_3^2]\chi_1^{(z)}.\end{aligned} \tag{35}$$

One can propose the solution $\chi_1^{(z)}$ as follows:

$$\chi_1^{(z)} = e^{ik_1x}e^{ik_3z}\mathrm{f}^{(z)}(y). \tag{36}$$

Along the same procedure used in the previous subsection, substituting back Eq. (36) into Eq. (35) brings us to Hermite's equation in which we have the eigenenergies given as

$$\omega^{(z)}_{n,k_3} = \sqrt{m^2 + (1-\lambda)^2 k_3^2 + 2n|eB|}. \tag{37}$$

We find that the solution of the Dirac field confined between two parallel plates in the space-like vector case of the $z$-direction for the right-moving field with positive value $eB$ is given as follows:

$$\psi^{(z)}_{k_1,n,k_3}(\boldsymbol{r}) = \frac{e^{ik_1x}e^{ik_3z}}{2\pi\sqrt{2\omega^{(z)}_{n,k_3}(\omega^{(z)}_{n,k_3}+m)}} \times \left[ C_1 \begin{pmatrix} (\omega_{n,k_3}+m)\mathrm{F}^{(z)}_{k_1,n}(y) \\ 0 \\ (1-\lambda)k_3\mathrm{F}^{(z)}_{k_1,n}(y) \\ \sqrt{2neB}\mathrm{F}^{(z)}_{k_1,n-1}(y) \end{pmatrix} + C_2 \begin{pmatrix} 0 \\ (\omega_{nk_3}+m)\mathrm{F}^{(z)}_{k_1,n-1}(y) \\ \sqrt{2neB}\mathrm{F}^{(z)}_{k_1,n}(y) \\ -(1-\lambda)k_3\mathrm{F}^{(z)}_{k_1,n-1}(y) \end{pmatrix} \right], \tag{38}$$

and

$$\psi^{(z)}_{k_1,0,k_3}(\boldsymbol{r}) = \frac{e^{ik_1x}e^{ik_3z}}{2\pi\sqrt{2\omega^{(z)}_{0,k_3}(\omega^{(z)}_{0,k_3}+m)}} C_0\mathrm{F}^{(z)}_{k_10}(y) \begin{pmatrix} \omega^{(z)}_{0,k_3}+m \\ 0 \\ (1-\lambda)k_3 \\ 0 \end{pmatrix}, \tag{39}$$

for $n \geq 1$ and $n = 0$, respectively, where

$$\mathrm{F}^{(z)}_{k_1,n}(y) = \sqrt{\frac{(eB)^{1/2}}{2^n n!\pi^{1/2}}} \exp\left[ -\frac{eB}{2}\left(y + \frac{k_1}{eB}\right)^2 \right] H_n\left[ \sqrt{eB}\left(y + \frac{k_1}{eB}\right) \right], \tag{40}$$

with the Hermite polynomial $H_n(y)$. In a similar way, we can obtain the solution for the left-moving field as follows:

$$\psi^{(+,z)}_{k_1,n,-k_3}(\boldsymbol{r}) = \frac{e^{ik_1x}e^{-ik_3z}}{2\pi\sqrt{2\omega^{(z)}_{n,k_3}(\omega^{(z)}_{n,k_3}+m)}} \times \left[ \tilde{C}_1 \begin{pmatrix} (\omega^{(z)}_{n,k_3}+m)\mathrm{F}^{(z)}_{k_1,n}(y) \\ 0 \\ -(1-\lambda)k_3\mathrm{F}^{(z)}_{k_1,n}(y) \\ \sqrt{2neB}\mathrm{F}^{(z)}_{k_1,n-1}(y) \end{pmatrix} + \tilde{C}_2 \begin{pmatrix} 0 \\ (\omega^{(z)}_{n,k_3}+m)\mathrm{F}^{(z)}_{k_1,n-1}(y) \\ \sqrt{2neB}\mathrm{F}^{(z)}_{k_1,n}(y) \\ (1-\lambda)k_3\mathrm{F}^{(z)}_{k_1,n-1}(y) \end{pmatrix} \right], \tag{41}$$

$$\psi^{(+,z)}_{k_1,0,-k_3}(\boldsymbol{r}) = \frac{e^{ik_1x}e^{-ik_3z}}{2\pi\sqrt{2\omega^{(z)}_{0,k_3}(\omega^{(z)}_{0,k_3}+m)}} \tilde{C}_0\mathrm{F}^{(z)}_{k_1,0}(y) \begin{pmatrix} \omega^{(z)}_{0,k_3}+m \\ 0 \\ -(1-\lambda)k_3 \\ 0 \end{pmatrix}, \tag{42}$$

for $n \geq 1$ and $n = 0$, respectively, where the eigenenergies $\omega^{(z)}_{n,k_3}$ are given by Eq. (37) (see Appendix A for the detailed derivation). The complex coefficients in the above Dirac field can be determined by similar orthonormality conditions given in Eq. (30). For the case of the negative energy solution, we derive it in detail in Appendix B.2.

We next write the total spatial solution for the Dirac field inside the confinement area as follows:

$$\psi^{(+,z)}_{k_1,n,k_3}(\boldsymbol{r}) = \psi^{(+,z)}_{k_1,n,k_3}(\boldsymbol{r}) + \psi^{(+,z)}_{k_1,n,-k_3}(\boldsymbol{r}). \tag{43}$$

For nonzero complex coefficients $C_1, C_2, \tilde{C}_1, \tilde{C}_2$, we have the constraint of the momentum $k_3$ as follows:

$$m\ell \sin(k_3\ell) + (1-\lambda)k_3\ell \cos(k_3\ell) = 0, \tag{44}$$

for arbitrary Landau level $n$. One can see that the parameter $\lambda$ affects the constraint while the magnetic field does not. The allowed momentum that satisfies the constraint (44) is $k_{3l}$ with $l = 0, 1, 2, 3, \cdots$. The discretized eigenenergies of the field under the MIT boundary can be written as follows:

$$\omega_{n,l}^{(z)} = \sqrt{m^2 + (1-\lambda)^2 k_{3l}^2 + 2n|eB|}. \tag{45}$$

Below we will compute the Casimir energy of the charged Dirac field under the presence of the MIT boundary. For this purpose, we write down the Hamiltonian density for the space-like vector case as follows:

$$\mathcal{H}^{(z)} = -\bar{\Psi}^{(z)}\big[i\gamma^j\partial_j - e\gamma^\mu A_\mu - m\big]\Psi^{(z)} = i\Psi^{(z)\dagger}\partial_0\Psi^{(z)}. \tag{46}$$

The vacuum energy reads

$$E_{\text{Vac.}} = -\frac{|eB|L^2}{\pi}\sum_{n=0}^{\infty}\sum_{l=1}^{\infty} i_n\sqrt{m^2 + (1-\lambda)^2\left(\frac{k'_{3l}}{\ell}\right)^2 + 2n|eB|}, \tag{47}$$

where we have used the eigenenergies given in Eq. (45) and $k'_{3\ell}(\equiv k_{3l}\ell)$. From the above vacuum energy, one can see that its value is divergent. To solve the issue, we employ the Abel–Plana-like summation as follows [56]:

$$\sum_{l=1}^{\infty}\frac{\pi\,\mathrm{f}_n(k'_{3l})}{\left(1-\frac{\sin(2k'_{3l})}{2k'_{3l}}\right)} = -\frac{\pi\, bm\mathrm{f}_n(0)}{2(bm+1)} + \int_0^\infty dz\mathrm{f}_n(z) - i\int_0^\infty dt\frac{\mathrm{f}_n(it)-\mathrm{f}_n(-it)}{\frac{t+bm}{t-bm}e^{2t}+1}. \tag{48}$$

From the momentum constraint in the space-like vector case (44), the denominator on the left-hand side of Eq. (48) can be rewritten in the following form:

$$1 - \frac{\sin(2k'_{3l})}{2k'_{3l}} = 1 + \frac{bm}{k'^2_{3l} + (bm)^2}, \tag{49}$$

where

$$b = \ell(1-\lambda)^{-1}. \tag{50}$$

Then, after applying the Abel–Plana-like summation to the vacuum energy, Eq. (47) becomes

$$E_{\text{Vac.}} = -\frac{|eB|L^2}{\pi^2 b}\sum_{n=0}^{\infty} i_n\Bigg[-\frac{\pi\, bm\mathrm{f}_n(0)}{2(bm+1)} + \int_0^\infty dq\mathrm{f}_n(q) - i\int_0^\infty dt\frac{\mathrm{f}_n(it)-\mathrm{f}_n(-it)}{\frac{t+bm}{t-bm}e^{2t}+1}\Bigg], \tag{51}$$

where the function $\mathrm{f}_n(q)$ is defined as

$$\mathrm{f}_n(q) = \sqrt{m^2b^2 + q^2 + 2n|eB|b^2}\left(1 + \frac{bm}{q^2+(bm)^2}\right). \tag{52}$$

Next, one can decompose the first and second terms in the vacuum energy (51) into two parts: (i) in the absence of the boundary conditions of two plates and (ii) in the presence of one plate. The latter part is irrelevant to our discussion because it does not contribute to the force. Then, the last term of Eq. (51) can be understood as the Casimir energy

$$E_{\text{Cas.}} = \frac{i|eB|L^2}{\pi^2 b}\sum_{n=0}^{\infty} i_n\int_0^\infty dt\frac{\mathrm{f}_n(it)-\mathrm{f}_n(-it)}{\frac{t+bm}{t-bm}e^{2t}+1}. \tag{53}$$

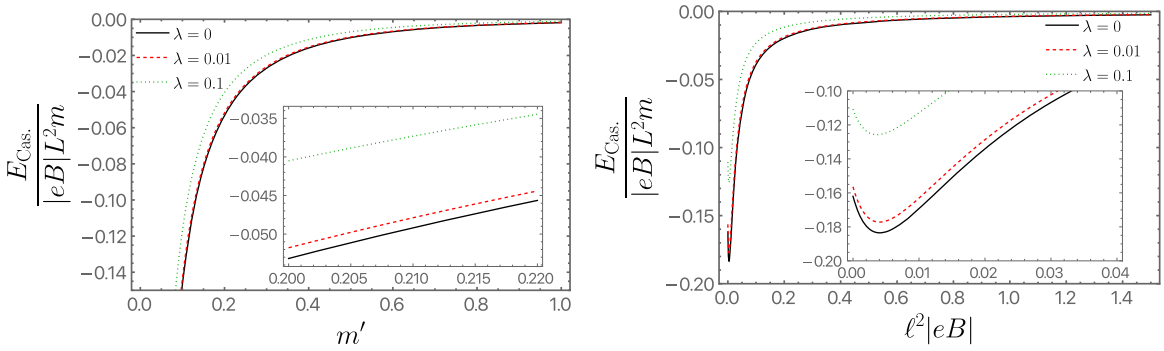


**Fig. 2.** (Left) The scaled Casimir energy of the space-like vector case as a function of the dimensionless parameter $m'$ for fixed $\ell^2|eB| = 2$. (Right) The scaled Casimir energy of the space-like vector case as a function of the dimensionless parameter $\ell^2|eB|$ for fixed $m' = 1$. In both panels, we use three different values of the parameter $\lambda = 0, 0.01, 0.1$.

Using Eq. (52) and introducing a variable of $t = bu$, the Casimir energy reads

$$E_{\rm Cas.} = -\frac{2|eB|L^2}{\pi^2}\sum_{n=0}^{\infty} i_n \int_0^{\infty} du\sqrt{u^2 - M_n^2}\left(\frac{b\,(u-m) - m/(m+u)}{(u+m)e^{2bu} + u - m}\right), \tag{54}$$

where

$$M_n = \sqrt{m^2 + 2n|eB|}. \tag{55}$$

The range of integration of Eq. (54) can be split into two intervals, i.e. $[0,\ M_n]$ and $[M_n,\ \infty]$. The integration result of the first interval vanishes while the second one remains. To proceed further with the Casimir energy, we next rewrite the following quantity as

$$\frac{b(u-m) - m/(m+u)}{(u+m)e^{2bu} + u - m} = -\frac{1}{2}\frac{d}{du}\ln\left(1 + \frac{u-m}{u+m}e^{-2bu}\right), \tag{56}$$

which leads the Casimir energy to

$$E_{\rm Cas.} = \frac{|eB|L^2}{\pi^2 b}\sum_{n=0}^{\infty} i_n \int_0^{\infty} dy\sqrt{y^2 + 2ybM_n}\frac{d}{dy}\ln\left(1 + \frac{y + b(M_n - m)}{y + b(M_n + m)}e^{-2(y+bM_n)}\right), \tag{57}$$

where we have introduced a new variable as

$$y = bu - bM_n. \tag{58}$$

Performing integration by part for Eq. (57), we finally find the simpler form of the Casimir energy as follows:

$$E_{\rm Cas.} = -\frac{|eB|L^2}{\pi^2 b} \times \sum_{n=0}^{\infty} i_n \int_0^{\infty} dy(y + bM_n)(y^2 + 2byM_n)^{-1/2}\ln\left(1 + \frac{y + b(M_n - m)}{y + b(M_n + m)}e^{-2(y+bM_n)}\right). \tag{59}$$

We next numerically evaluate the expression of the Casimir energy given in Eq. (59). The left panel of Fig. 2 depicts the scaled Casimir energy as a function of the dimensionless parameter $m'$ ($\equiv m\ell$) for various values of the parameter $\lambda = 0, 0.01, 0.1$ with a fixed parameter $\ell^2|eB| = 2$. From this figure, we find that the scaled Casimir energy converges to zero as the parameter $m'$ becomes larger. The right panel of Fig. 2 depicts the scaled Casimir energy as a function of the dimensionless parameter $\ell^2|eB|$ for a fixed parameter $m' = 1$. From this figure, one can

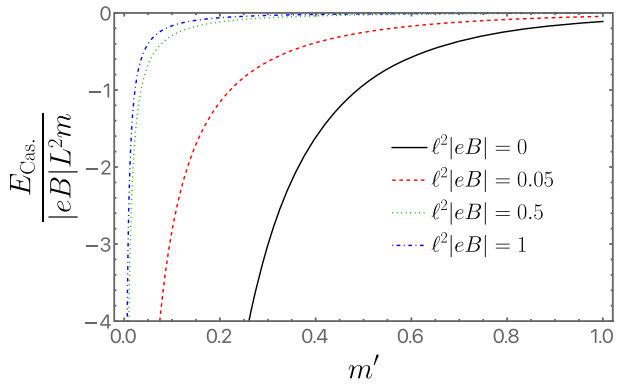


**Fig. 3.** The scaled Casimir energy of the space-like vector case as a function of the dimensionless parameter $m'$ ($\equiv m\ell$) for various values of the parameter $\ell^2|eB| = 0, 0.05, 0.5, 1$ and the fixed parameter $\lambda = 0.1$.

see that the scaled Casimir energy also generally converges to zero as the parameter $\ell^2|eB|$ increases. However, in the small region of $\ell^2|eB|$ ($\ell^2|eB| < 0.005$), the behavior of the scaled Casimir energy is not trivial. This can be understood from the formula in Eq. (60) when we take the vanishing magnetic field $B \to 0$. This nontrivial behavior also appears in Ref. [22], where the authors have discussed the Casimir energy of the fermion field in the framework of standard quantum field theory (preserved Lorentz symmetry). Both panels of Fig. 2 show that as the parameter $\lambda$ increases, the magnitude of the Casimir energy will decrease and vice versa, as previously shown by Ref. [33] for the absence of the magnetic field. Figure 3 plots the scaled Casimir energy as a function of the dimensionless parameter $m'$ for various values of the parameter $\ell^2|eB| = 0, 0.05, 0.5, 1$ and the fixed parameter $\lambda = 0.1$. One can see that increasing $\ell^2|eB|$ leads to the converging of the Casimir energy to zero.

In the rest of this part, we investigate the approximate cases of the Casimir energy. In the case of the weak magnetic field $\ell^2|eB| \ll 1$, the above Casimir energy (59) for an arbitrary $m'$ ($\equiv m\ell$) reduces to

$$E_{\text{Cas.}} \simeq -\frac{L^2}{\pi^2 b^3}\int_{bm}^{\infty} dx x^2 \int_0^{\infty} dv(v+1)\frac{1}{\sqrt{v(v+2)}} \ln\left(1 + \frac{x(v+1) - bm}{x(v+1) + bm} e^{-2x(v+1)}\right). \quad (60)$$

To obtain the above expression, we have used the replacement of summation with integration, $v = y/(bM_n)$, and $x = bM_n$. Taking the case of light mass $m' \ll 1$ for Eq. (60), we recover the earlier result by Ref. [33] as follows:

$$E_{\text{Cas.}} \simeq -\frac{7\pi^2(1-\lambda)^3 L^2}{2880\ell^3}\left[1 - \frac{120m'}{7\pi^2(1-\lambda)}\right], \quad (61)$$

where we have expanded the integrand up to the order of $\mathcal{O}(m')$ and omitted the higher ones. The first term corresponds to the Casimir energy in the massless case with the effect of the Lorentz violation, whereas the second term corresponds to the correction part. In the case of preserved Lorentz symmetry, $\lambda = 0$, we recover the well-known Casimir energy of the massless fermion derived by Johnson [16].

To obtain the approximated result of Eq. (61), one can also start from the general Casimir energy (59) and take its light mass case $m' \ll 1$ for the arbitrary magnetic field as

$$E_{\text{Cas.}} \simeq -\frac{|eB|L^2}{\pi^2 b}\sum_{n=0}^{\infty} i_n \int_0^{\infty} dy \left[ \frac{(y+b\sqrt{2neB})\ln\left(1+e^{-2(y+b\sqrt{2neB})}\right)}{\sqrt{y^2+2yb\sqrt{2neB}}} - \frac{2bme^{-2(y+b\sqrt{2neB})}}{\sqrt{y^2+2yb\sqrt{2neB}}(1+e^{-2(y+b\sqrt{2neB})})} \right]. \tag{62}$$

Then, taking the limit of the weak magnetic field, the above expression reduces to Eq. (61).

In the case of heavy mass $m' \gg 1$, we find that the Casimir energy approximately reduces to

$$E_{\text{Cas.}} \simeq -\frac{|eB|L^2(1-\lambda)^{3/2}}{16\pi^{3/2}\ell\sqrt{m'}}\sum_{n=0}^{\infty} i_n e^{\frac{-2\sqrt{m'^2+2nB'}}{(1-\lambda)}}, \tag{63}$$

where we have expanded the integrand of Eq. (59) up to the order of $\mathcal{O}(1/m')$ and omitted the higher ones. In the case of the weak magnetic field $\ell^2|eB| \ll 1$, the above Casimir energy (63) reads

$$E_{\text{Cas.}} \simeq -\frac{L^2(1-\lambda)^{5/2}\sqrt{m'}}{32\pi^{3/2}\ell^3} e^{-\frac{2m'}{(1-\lambda)}}. \tag{64}$$

We can see that, in the case of heavy mass, the Casimir energy goes to zero as the mass increases.

We next investigate the Casimir energy in the case of the strong magnetic field $\ell^2 eB \gg 1$. In this case, together with light mass $m' \ll 1$, the Casimir energy in Eq. (59) approximately reduces to

$$E_{\text{Cas.}} \simeq -\frac{|eB|L^2(1-\lambda)}{48\ell}. \tag{65}$$

Meanwhile for the case of the strong magnetic field $\ell^2|eB| \gg 1$ and taking the limit of heavy mass $m' \gg 1$, the Casimir energy reads

$$E_{\text{Cas.}} \simeq -\frac{|eB|L^2(1-\lambda)^{3/2}}{32\pi^{3/2}\ell\sqrt{m'}} e^{\frac{-2m'}{(1-\lambda)}}. \tag{66}$$

From the above expression, we note that the Casimir energy converges to zero with the increase of parameter $m'$. Based on the above result, we can investigate the role of the magnetic field by computing the ratio of the Casimir energy in the case of the strong magnetic field to the weak one as follows:

$$\frac{E_{\text{Cas}}(\ell^2|eB| \gg 1)}{E_{\text{Cas}}(\ell^2|eB| \ll 1)} = \frac{60|eB|\ell^2}{7\pi^2(1-\lambda)^2}, \quad \text{for } m' \ll 1, \tag{67}$$

$$\frac{E_{\text{Cas}}(\ell^2|eB| \gg 1)}{E_{\text{Cas}}(\ell^2|eB| \ll 1)} = \frac{2e^{\frac{-2m'}{(1-\lambda)}}}{\sum_{n=0}^{\infty} i_n e^{\frac{-2\sqrt{m'^2+2n\ell^2 eB}}{(1-\lambda)}}}, \quad \text{for } m' \gg 1. \tag{68}$$

It can be inferred from the above expressions that the magnetic field increases the Casimir energy. In such cases, we can also see that the roles of the Lorentz violation scale the plate's distance.

To end this section, let us compare qualitatively the Casimir energy formulation of both scalar and fermion fields under Lorentz violation and a magnetic field background. The case of the scalar field has been studied with Dirichlet and mixed (Dirichlet–Neumann) boundary conditions in Refs. [29,67]. For the present work, we study the fermion field under the boundary condition of the MIT bag model. In comparison to Refs. [29,67], we note that their method of

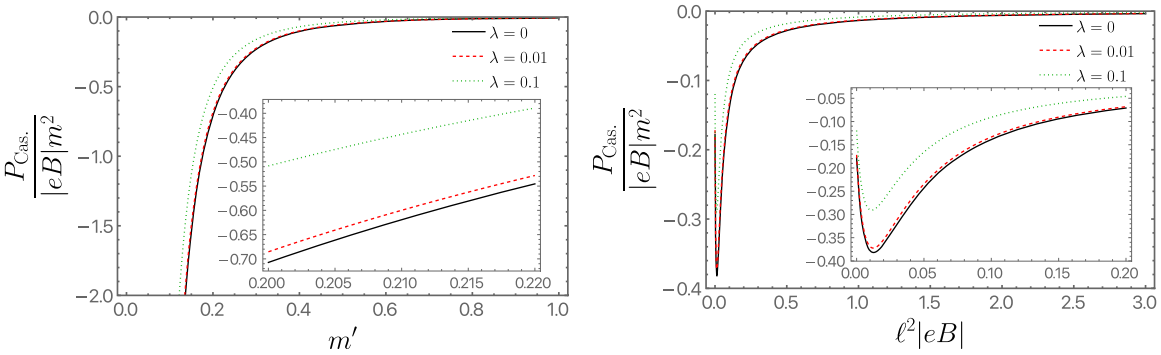


**Fig. 4.** (Left) The scaled Casimir pressure of the space-like vector case as a function of the dimensionless parameter $m'$ for fixed $\ell^2|eB| = 2$. (Right) The scaled Casimir pressure of the space-like vector case as a function of the dimensionless parameter $\ell^2|eB|$ for fixed $m' = 1$. In both panels, we use the various values of the parameter $\lambda = 0, 0.01, 0.1$.

deriving the Casimir energy differs from ours, where they used the zeta function regularization technique to tackle the infinitive issue. Besides that, their plate's distances are scaled differently. Namely, it is scaled by $(1-\lambda)^{1/2}$ whereas ours is scaled by $(1-\lambda)$. In the large mass limit and strong magnetic limit, the resulting Casimir energies are consistent with Refs. [29,67]. In particular, the magnetic field $|eB|$ appears linearly in the front factor of the Casimir energy.[3] The quantitative difference between the Casimir energy of the scalar and Dirac fields using the Abel–Plana formula generally appears as a statistical factor, as shown by Ref. [21]. In particular, we have an exponential factor $(\frac{t+bm}{t-bm}e^{2t}+1)^{-1}$ for the fermion field in our result (see Eq. (53)). In comparison to Ref. [21], it is consistent in the case of preserved Lorentz symmetry ($\lambda = 0$).

## 4. Casimir pressure

In this section, we investigate the Casimir pressure for the space-like vector case. It can be obtained from the Casimir energy (59) by taking the derivative with respect to the plate's distance as

$$\begin{aligned} P_{\rm Cas.} &= -\frac{1}{L^2}\frac{\partial E_{\rm Cas.}}{\partial \ell} \\ &= -\sum_{n=0}^{\infty} i_n \int_0^{\infty} dy \frac{1}{(1-\lambda)b^2\pi^2(y(2bM_n+y))^{3/2}} \\ &\quad \times eBy\left\{\frac{2b(bM_n+y)(2bM_n+y)(b^2M_n(M_n^2-m^2)+2bM_n^2y+y(m+M_ny))}{b^2(M_n^2-m^2)+2bM_ny+y^2+e^{2(bM_n+y)}(b(m+M_n)+y)^2}\right. \\ &\quad \left.+(b^2M_n^2+3bM_ny+y^2)\ln\left(1+\frac{e^{-2(bM_n+y)}(b(-m+M_n)+y)}{b(m+M_n)+y}\right)\right\}. \end{aligned} \tag{69}$$

We plot the behavior of the scaled Casimir pressure in Figs. 4 and 5. In general, we can see that its behavior is similar to that of the Casimir energy. From the left panel of Fig. 4, one can see the scaled Casimir pressure converges to zero as the parameter $m'$ increases; whereas, from the right panel, it generally converges to zero with the increasing of $\ell^2|eB|$. However, for a small region of $\ell^2|eB|$ ($\ell^2|eB| < 0.02$), its behavior is not trivial. We can also understand this behavior with a similar argument to that used for the scaled Casimir energy discussed in

[3] We should take the large mass limit of the Casimir energy Eq. (49) mentioned is that in Ref. [29] and not that in the present work.

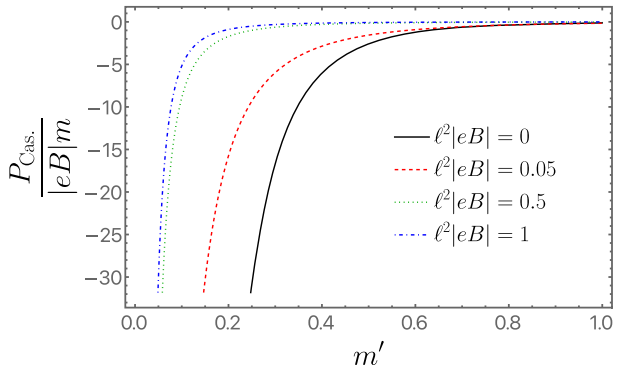


**Fig. 5.** The scaled Casimir pressure of the space-like vector case as a function of the dimensionless parameter $m'$ ($\equiv m\ell$) for various values of parameter $\ell^2|eB| = 0, 0.05, 0.5, 1$ and fixed $\lambda = 0.1$.

the previous subsection and the explicit expression is given below (Eq. (70)). Both panels of Fig. 4 show that the magnitude of the Casimir pressure decreases as the parameter $\lambda$ increases. Figure 5 plots the scaled Casimir pressure as a function of parameter $m'$ with various values of $\ell^2|eB|$ and fixed parameter $\lambda = 0.1$. From this figure, we can see that the scaled Casimir pressure converges to zero with the increasing of parameters $m'$ and $\ell^2|eB|$ and it supports the behavior shown in Fig. 4.

We next investigate the Casimir pressure in the cases of weak and strong magnetic fields. In the case of the weak magnetic field $\ell^2|eB| \ll 1$, the Casimir pressure (69) approximately reduces to

$$P_{\text{Cas.}} \simeq -\frac{1}{(1-\lambda)b^4\pi^2} \times \int_{bm}^{\infty} dx \int_0^{\infty} dv \frac{x^2}{v^{1/2}(2+v)^{3/2}} \left( \frac{2x(1+v)(2+v)(x^2(1+v)^2 + tbm - (bm)^2)}{x^2(1+v)^2 - (bm)^2 + e^{2x(1+v)}(bm + x(1+v))^2} + (1+3v+v^2)\ln\left(1 + \frac{e^{-2x(1+v)}(-bm + x(1+v))}{(bm + x(1+v))}\right)\right). \tag{70}$$

We further take the light mass limit $m' \ll 1$ for the above expression, then we have

$$P_{\text{Cas.}} \simeq -\frac{(1-\lambda)^2(7\pi^2(1-\lambda) - 80m')}{960\ell^4}, \tag{71}$$

which covers the earlier result of Ref. [33]. As discussed in the previous section, to obtain the above expression we can use the reverse way, namely, taking its light mass limit and then considering the weak magnetic field.

The Casimir pressure for the case of light mass with an arbitrary magnetic field is approximately given as follows:

$$P_{\text{Cas.}} \simeq P^{(0)}_{\text{Cas.}} + P^{(1)}_{\text{Cas.}}, \tag{72}$$

where $P^{(0)}_{\text{Cas.}}$ is the Casimir pressure for the massless case explicitly given as

$$P^{(0)}_{\text{Cas.}} = -\sum_{n=0}^{\infty} i_n \int_0^{\infty} dy \frac{|eB|y}{b^2\pi^2(1-\lambda)\left(y\left(2b\sqrt{2neB}+y\right)\right)^{3/2}} \times \left\{ \frac{2b\sqrt{2neB}\left(2b\sqrt{2neB}+y\right)\left(b\sqrt{2neB}+y\right)}{\left(1+e^{2\left(b\sqrt{2neB}+y\right)}\right)} + \left(b^2 2neB + 3b\sqrt{2neB}y + y^2\right)\ln\left(1+e^{-2\left(b\sqrt{2neB}+y\right)}\right)\right\}, \tag{73}$$

and $P^{(1)}_{\text{Cas.}}$ is the first-order correction to the Casimir pressure $\mathcal{O}(m')$ explicitly given as

$$P^{(1)}_{\text{Cas.}} = \sum_{n=0}^{\infty} i_n \int_0^{\infty} dy \frac{2|eB|yb\sqrt{2neB}\left(1+e^{2\left(b\sqrt{2neB}+y\right)}(1+2y)+4e^{2\left(b\sqrt{2neB}+y\right)}b\sqrt{2neB}\right)bm}{b^2\pi^2\left(1+e^{2\left(b\sqrt{2neB}+y\right)}\right)^2\left(y\left(y+2b\sqrt{2neB}\right)\right)^{3/2}(1-\lambda)}. \tag{74}$$

We next investigate the Casimir pressure (69) in the case of heavy mass $m' \gg 1$. In this case, we have

$$P_{\text{Cas.}} \simeq -\frac{|eB|\sqrt{m'}}{(1-\lambda)^{1/2}8\pi^{3/2}b^2}\sum_{n=0}^{\infty} i_n e^{-2\sqrt{m'^2+2neB}}, \tag{75}$$

and with the limit of the weak magnetic field $\ell^2|eB| \ll 1$, the above Casimir pressure approximately reduces to

$$P_{\text{Cas.}} \simeq -\frac{(1-\lambda)^{5/2}m'^{3/2}}{16\pi^{3/2}\ell^4}e^{-\frac{2m'}{(1-\lambda)}}. \tag{76}$$

Showing similar behavior to the Casimir energy (66), one can see that the Casimir pressure in the limit of heavy mass (75) converges to zero as the particle's mass increases.

Based on the results of the Casimir pressure in the cases of light (72) and heavy masses (75), we will analyze the behavior in the strong magnetic field. Taking the limit of the strong magnetic field $\ell^2|eB| \gg 1$ for Eq. (72), the Casimir pressure approximately reduces to

$$P_{\text{Cas.}} \simeq -\frac{|eB|(1-\lambda)}{48\ell^2}, \tag{77}$$

while for Eq. (75), we obtain

$$P_{\text{Cas.}} \simeq -\frac{|eB|(1-\lambda)^{3/2}\sqrt{m'}}{16\pi^{3/2}\ell^2}e^{\frac{-2m'}{(1-\lambda)}}. \tag{78}$$

One can also derive both of the above equations by taking the derivative of the Casimir energy (Eqs. (65) and (66)) with respect to the plate's distance. In the same way as with the Casimir energy, we can also analyze the role of the strong magnetic field by computing the ratio of the Casimir pressure in the case of the strong magnetic field to the weak one as follows:

$$\frac{P_{\text{Cas.}}(\ell^2|eB| \gg 1)}{P_{\text{Cas.}}(\ell^2|eB| \ll 1)} = \frac{20|eB|\ell^2}{7\pi^2(1-\lambda)^2}, \quad \text{for } m' \ll 1, \tag{79}$$

$$\frac{P_{\text{Cas.}}(\ell^2|eB| \gg 1)}{P_{\text{Cas.}}(\ell^2|eB| \ll 1)} = \frac{2e^{\frac{-2m'}{(1-\lambda)}}}{\sum_{n=0}^{\infty} i_n e^{\frac{-2\sqrt{m'^2+2\ell^2 eB}}{(1-\lambda)}}}, \quad \text{for } m' \gg 1. \tag{80}$$

From the above expressions, we can see that the magnetic field increases the Casimir pressure.

## 5. Summary

We have studied the Casimir effect of a Lorentz-violating Dirac field with a background uniform magnetic field. In the model, the Lorentz violation is described by two parameters: (i) $\lambda$, which determines the intensity of the violation; and (ii) vector $u^\mu$, which determines the direction of the violation. In the present study, we investigated two vector cases, namely, time-like and space-like vector cases. For the space-like vector case, we only discussed the $z$-direction. The purpose of the study is to find the effect of the Lorentz violation parameter $\lambda$ together with the presence of the magnetic field on the behavior of the Casimir energy as well as its pressure. We used the boundary condition from the MIT bag model [14–16] to represent the property of the plates. From our derivation, we find that for the time-like vector case, the magnetic field and the Lorentz violating parameter do not affect the structure of the momentum constraint, whereas for the space-like vector case, only the Lorentz violating parameter appears.

We noted that the vacuum energy under the MIT boundary condition is divergent. Using Abel–Plana like summation [56], we can extract this vacuum energy into three main parts, namely, vacuum energy in the absence of a boundary condition, vacuum energy in the presence of a single boundary condition that is not relevant to the Casimir effect, and the term for the rest that refers to the Casimir energy. We can derive the Casimir energy by subtracting the vacuum energy in the presence of the boundary condition from that in the absence of one. The Lorentz violation for the time-like vector case does not affect the structure of the Casimir energy or its pressure, whereas for the space-like vector case, the violation affects it. We also found that the magnetic field has an effect on the Casimir energy and the pressure for both time-like and space-like vector cases.

We have demonstrated the behavior of the scaled Casimir energy and the pressure as a function of mass, the parameter $\lambda$, and magnetic field. For the fixed parameter $\lambda$ and magnetic field, the scaled Casimir energy (pressure) converges to zero with the increase of mass (see the left panel of Figs. 2 and 4). For fixed parameter $\lambda$ and mass, the scaled Casimir energy (pressure) converges to zero with the increase of mass (see the left panel of Fig. 2 converge to zero with the increasing of the magnetic field; see also the right panel of Figs. 2 and 4). We also found that the increase of the parameter $\lambda$ leads to the increase of the Casimir energy and the pressure, as has been pointed out by Ref. [33]. Lastly, we computed the ratio of the Casimir energy and its pressure in the case of the strong magnetic field to those in the case of the weak magnetic field. As a result, we found that the strong magnetic field increases the Casimir energy and its pressure.

For future work, it would be interesting to discuss the thermal effect in a similar setup to our present work (cf. Ref. [67] for the scalar field). It would also be interesting to study a similar setup under the general boundary, e.g. chiral MIT boundary conditions [18].

**Acknowledgements**

A. Rohim was partly supported by Hibah Riset FMIPA UI under contract No. PKS-025/UN2.F3.D/PPM.00.02/2023. This work was started when A. Rohim belonged to the National Research and Innovation Agency (BRIN), Indonesia, as a postdoctoral fellow and was completed after his moving to Universitas Indonesia as a lecturer.

## Funding

Open Access funding: SCOAP[3].

## Appendix A. Detailed derivation of the constraint for momentum

In this section, we provide the complementary derivation of the momentum constraint. Applying the boundary condition from the MIT bag model (6) to the solution of the Dirac equation, we have two equations as follows:

$$i\sigma^3\chi_2|_{z=0} - \chi_1|_{z=0} = 0, \tag{A1}$$

$$i\sigma^3\chi_2|_{z=\ell} + \chi_1|_{z=\ell} = 0, \tag{A2}$$

where we have used $n_\mu^{(0)} = (0, 0, 0, 1)$ and $n_\mu^{(\ell)} = (0, 0, 0, -1)$ at the first $z = 0$ and second plates $z = \ell$, respectively. Then, in a more explicit expression, we have four equations for boundary conditions as follows:

$$i\chi_{21}|_{z=0} - \chi_{11}|_{z=0} = 0, \tag{A3}$$

$$i\chi_{22}|_{z=0} + \chi_{12}|_{z=0} = 0, \tag{A4}$$

$$i\chi_{21}|_{z=\ell} + \chi_{11}|_{z=\ell} = 0, \tag{A5}$$

$$i\chi_{22}|_{z=\ell} - \chi_{12}|_{z=\ell} = 0, \tag{A6}$$

where we have decomposed the two-component spinors $\chi_1$ and $\chi_2$ as

$$\chi_1 = \begin{pmatrix} \chi_{11} \\ \chi_{12} \end{pmatrix}, \tag{A7}$$

$$\chi_2 = \begin{pmatrix} \chi_{21} \\ \chi_{22} \end{pmatrix}. \tag{A8}$$

The boundary conditions of Eqs. (A3–A6) can be simultaneously written in the form of multiplication between two matrices as follows:

$$\begin{pmatrix} \mathcal{P}_{11} & \mathcal{P}_{12} \\ \mathcal{P}_{21} & \mathcal{P}_{22} \end{pmatrix} \begin{pmatrix} C_0 \\ \tilde{C}_0 \end{pmatrix} = 0, \quad \text{for} \quad n = 0, \tag{A9}$$

and

$$\begin{pmatrix} \mathcal{Q}_{11} & \mathcal{Q}_{12} & \mathcal{Q}_{13} & \mathcal{Q}_{14} \\ \mathcal{Q}_{21} & \mathcal{Q}_{22} & \mathcal{Q}_{23} & \mathcal{Q}_{24} \\ \mathcal{Q}_{31} & \mathcal{Q}_{32} & \mathcal{Q}_{33} & \mathcal{Q}_{34} \\ \mathcal{Q}_{41} & \mathcal{Q}_{42} & \mathcal{Q}_{43} & \mathcal{Q}_{44} \end{pmatrix} \begin{pmatrix} C_1 \\ C_2 \\ \tilde{C}_1 \\ \tilde{C}_2 \end{pmatrix} = 0, \quad \text{for} \quad n \geq 1, \tag{A10}$$

where the matrix elements are given by

$$\mathcal{P}_{11}^{(t)} = ik_3 - ((1+\lambda)\omega_{0k_3}^{(t)} + m), \tag{A11}$$

$$\mathcal{P}_{12}^{(t)} = -ik_3 - ((1+\lambda)\omega_{0k_3}^{(t)} + m), \tag{A12}$$

$$\mathcal{P}_{21}^{(t)} = [ik_3 + ((1+\lambda)\omega_{0k_3}^{(t)} + m)]e^{ik_3\ell}, \tag{A13}$$

$$\mathcal{P}_{22}^{(t)} = [-ik_3 + ((1+\lambda)\omega_{0k_3}^{(t)} + m)]e^{-ik_3\ell}, \tag{A14}$$

$$\mathcal{Q}_{11}^{(t)} = -\mathcal{Q}_{22}^{(t)} = ik_3 - ((1+\lambda)\omega_{nk_3}^{(t)} + m), \tag{A15}$$

$$\mathcal{Q}_{12}^{(t)} = \mathcal{Q}_{14}^{(t)} = \mathcal{Q}_{21}^{(t)} = \mathcal{Q}_{23}^{(t)} = i\sqrt{2neB}, \tag{A16}$$

$$\mathcal{Q}_{13}^{(t)} = -\mathcal{Q}_{24}^{(t)} = -ik_3 - ((1+\lambda)\omega_{nk_3}^{(t)} + m), \tag{A17}$$

$$\mathcal{Q}_{31}^{(t)} = -\mathcal{Q}_{42}^{(t)} = [ik_3 + ((1+\lambda)\omega_{nk_3}^{(t)} + m)]e^{ik_3\ell}, \tag{A18}$$

$$\mathcal{Q}_{32}^{(t)} = \mathcal{Q}_{41}^{(t)} = i\sqrt{2neB}e^{ik_3\ell}, \tag{A19}$$

$$\mathcal{Q}_{34}^{(t)} = \mathcal{Q}_{43}^{(z)} = i\sqrt{2neB}e^{-ik_3\ell}, \tag{A20}$$

$$\mathcal{Q}_{33}^{(t)} = -\mathcal{Q}_{44}^{(t)} = [-ik_3 + ((1+\lambda)\omega_{nk_3}^{(t)} + m)]e^{-ik_3\ell}, \tag{A21}$$

and

$$\mathcal{P}_{11}^{(z)} = i(1-\lambda)k_3 - (\omega_{0k_3}^{(z)} + m), \tag{A22}$$

$$\mathcal{P}_{12}^{(z)} = -i(1-\lambda)k_3 - (\omega_{0k_3}^{(z)} + m), \tag{A23}$$

$$\mathcal{P}_{21}^{(z)} = [i(1-\lambda)k_3 + (\omega_{0k_3}^{(z)} + m)]e^{ik_3\ell}, \tag{A24}$$

$$\mathcal{P}_{22}^{(z)} = [-i(1-\lambda)k_3 + (\omega_{0k_3}^{(z)} + m)]e^{-ik_3\ell}, \tag{A25}$$

$$\mathcal{Q}_{11}^{(z)} = -\mathcal{Q}_{22}^{(z)} = i(1-\lambda)k_3 - (\omega_{nk_3}^{(z)} + m), \tag{A26}$$

$$\mathcal{Q}_{12}^{(z)} = \mathcal{Q}_{14}^{(z)} = \mathcal{Q}_{21}^{(z)} = \mathcal{Q}_{23}^{(z)} = i\sqrt{2neB}, \tag{A27}$$

$$\mathcal{Q}_{13}^{(z)} = -\mathcal{Q}_{24}^{(z)} = -i(1-\lambda)k_3 - (\omega_{nk_3}^{(z)} + m), \tag{A28}$$

$$\mathcal{Q}_{31}^{(z)} = -\mathcal{Q}_{42}^{(z)} = [i(1-\lambda)k_3 + (\omega_{nk_3}^{(z)} + m)]e^{ik_3\ell}, \tag{A29}$$

$$\mathcal{Q}_{32}^{(z)} = \mathcal{Q}_{41}^{(z)} = i\sqrt{2neB}e^{ik_3\ell}, \tag{A30}$$

$$\mathcal{Q}_{34}^{(z)} = \mathcal{Q}_{43}^{(z)} = i\sqrt{2neB}e^{-ik_3\ell}, \tag{A31}$$

$$\mathcal{Q}_{33}^{(z)} = -\mathcal{Q}_{44}^{(z)} = [-i(1-\lambda)k_3 + (\omega_{nk_3}^{(z)} + m)]e^{-ik_3\ell}, \tag{A32}$$

for time-like and space-like vector cases in the $z$-direction, respectively. For arbitrary nonzero complex coefficients $C_0$, $\tilde{C}_0$, $C_1$, $C_2$, $\tilde{C}_1$, $\tilde{C}_2$, the vanishing of the determinant of the $2 \times 2$ matrix of Eq. (A9) and $4 \times 4$ matrices of Eq. (A10) is required, which leads to the constraint for momentum $k_3$.

## Appendix B. Negative-energy solutions

### *B.1. Time-like vector case*

The negative energy solution for the right-moving field component is as follows:

$$\psi^{(-,t)}_{k_1,n,k_3}(\boldsymbol{r}) = \frac{e^{-ik_1x}e^{-ik_3z}}{2\pi\sqrt{2(1+\lambda)\omega^{(t)}_{n,k_3}((1+\lambda)\omega^{(t)}_{n,k_3}+m)}} \times\left[\tilde{C}_1\begin{pmatrix} k_3\mathrm{f}^{(t)}_{-k_1n}(y) \\ -\sqrt{2neB}\mathrm{f}^{(t)}_{-k_1n-1}(y) \\ ((1+\lambda)\omega^{(t)}_{nk_3}+m)\mathrm{f}^{(t)}_{-k_1n}(y) \\ 0 \end{pmatrix} + \tilde{C}_2\begin{pmatrix} -\sqrt{2neB}\mathrm{f}^{(t)}_{-k_1n}(y) \\ -k_3\mathrm{f}^{(t)}_{-k_1n-1}(y) \\ 0 \\ ((1+\lambda)\omega^{(t)}_{nk_3}+m)\mathrm{f}^{(t)}_{-k_1n-1}(y) \end{pmatrix}\right], \tag{B1}$$

and

$$\psi^{(-,t)}_{k_1,0,k_3}(\boldsymbol{r}) = \frac{e^{-ik_1x}e^{-ik_3z}}{2\pi\sqrt{2(1+\lambda)\omega^{(t)}_{0,k_3}((1+\lambda)\omega^{(t)}_{0,k_3}+m)}}\tilde{C}_0\mathrm{f}^{(t)}_{-k_1,0}(y)\begin{pmatrix} k_3 \\ 0 \\ (1+\lambda)\omega^{(t)}_{0,k_3}+m \\ 0 \end{pmatrix}, \tag{B2}$$

for $n \geq 1$ and $n = 0$, respectively. The negative energy solution for the left-moving field component is as follows:

$$\psi^{(-,t)}_{k_1,n,-k_3}(\boldsymbol{r}) = \frac{e^{-ik_1x}e^{ik_3z}}{2\pi\sqrt{2(1+\lambda)\omega^{(t)}_{n,k_3}((1+\lambda)\omega^{(t)}_{n,k_3}+m)}} \times\left[C_1\begin{pmatrix} -k_3\mathrm{f}^{(t)}_{-k_1n}(y) \\ -\sqrt{2neB}\mathrm{f}^{(t)}_{-k_1n-1}(y) \\ ((1+\lambda)\omega^{(t)}_{nk_3}+m)\mathrm{f}^{(t)}_{-k_1n}(y) \\ 0 \end{pmatrix} + C_2\begin{pmatrix} -\sqrt{2neB}\mathrm{f}^{(t)}_{-k_1n}(y) \\ k_3\mathrm{f}^{(t)}_{-k_1n-1}(y) \\ 0 \\ ((1+\lambda)\omega^{(t)}_{nk_3}+m)\mathrm{f}^{(t)}_{-k_1n-1}(y) \end{pmatrix}\right], \tag{B3}$$

and

$$\psi^{(-,t)}_{k_1,0,-k_3}(\boldsymbol{r}) = \frac{e^{-ik_1x}e^{ik_3z}}{2\pi\sqrt{2(1+\lambda)\omega^{(t)}_{0,k_3}((1+\lambda)\omega^{(t)}_{0,k_3}+m)}}C_0\mathrm{f}^{(t)}_{-k_1,0}(y)\begin{pmatrix} -k_3 \\ 0 \\ (1+\lambda)\omega^{(t)}_{0,k_3}+m \\ 0 \end{pmatrix}, \tag{B4}$$

for $n \geq 1$ and $n = 0$, respectively. The total spatial solution inside the confinement area is given by the linear combination of the left- and right-moving field components as follows:

$$\psi^{(-,t)}_{k_1,n,l}(\boldsymbol{r}) = \psi^{(-,t)}_{k_1,n,k_{3l}}(\boldsymbol{r}) + \psi^{(-,t)}_{k_1,n,-k_{3l}}(\boldsymbol{r}), \tag{B5}$$

where we use $k_{3l}$ to represent the allowed momentum in the system.

*B.2. Space-like vector case (z-direction)*

The negative energy solutions for the right-moving field component are given as follows:

$$\psi^{(-,z)}_{k_1,n,k_3}(\boldsymbol{r}) = \frac{e^{-ik_1x}e^{-ik_3z}}{2\pi\sqrt{2\omega^{(z)}_{n,k_3}(\omega^{(z)}_{n,k_3}+m)}} \times\left[\tilde{C}_1\begin{pmatrix}(1-\lambda)k_3\mathrm{F}^{(z)}_{-k_1,n}(y)\\ -\sqrt{2neB}\mathrm{F}^{(z)}_{-k_1,n-1}(y)\\ (\omega^{(z)}_{n,k_3}+m)\mathrm{F}^{(z)}_{-k_1,n}(y)\\ 0\end{pmatrix}+\tilde{C}_2\begin{pmatrix}-\sqrt{2neB}\mathrm{F}^{(z)}_{-k_1,n}(y)\\ -(1-\lambda)k_3\mathrm{F}^{(z)}_{-k_1,n-1}(y)\\ 0\\ (\omega^{(z)}_{nk_3}+m)\mathrm{F}^{(z)}_{-k_1,n-1}(y)\end{pmatrix}\right], \tag{B6}$$

and

$$\psi^{(-,z)}_{k_1,0,k_3}(\boldsymbol{r}) = \frac{e^{-ik_1x}e^{-ik_3z}}{2\pi\sqrt{2\omega^{(z)}_{0,k_3}(\omega^{(z)}_{0,k_3}+m)}}\tilde{C}_0\mathrm{F}^{(z)}_{-k_1,0}(y)\begin{pmatrix}(1-\lambda)k_3\\ 0\\ \omega^{(z)}_{0,k_3}+m\\ 0\end{pmatrix}, \tag{B7}$$

for $n \geq 1$ and $n = 0$, respectively, where

$$\mathrm{f}^{(t)}_{-k_1,n}(y) = \sqrt{\frac{(eB)^{1/2}}{2^n n!\pi^{1/2}}}\exp\left[-\frac{eB}{2}\left(y-\frac{k_1}{eB}\right)^2\right]H_n\left[\sqrt{eB}\left(y-\frac{k_1}{eB}\right)\right]. \tag{B8}$$

The negative energy solutions for the left-moving field component are given as follows:

$$\psi^{(-,z)}_{k_1,n,-k_3}(\boldsymbol{r}) = \frac{e^{-ik_1x}e^{ik_3z}}{2\pi\sqrt{2\omega^{(z)}_{n,k_3}(\omega^{(z)}_{n,k_3}+m)}} \times\left[C_1\begin{pmatrix}-(1-\lambda)k_3\mathrm{F}^{(z)}_{-k_1,n}(y)\\ -\sqrt{2neB}\mathrm{F}^{(z)}_{-k_1,n-1}(y)\\ (\omega^{(z)}_{n,k_3}+m)\mathrm{F}^{(z)}_{-k_1,n}(y)\\ 0\end{pmatrix}+C_2\begin{pmatrix}-\sqrt{2neB}\mathrm{F}^{(z)}_{-k_1,n}(y)\\ (1-\lambda)k_3\mathrm{F}^{(z)}_{-k_1,n-1}(y)\\ 0\\ (\omega^{(z)}_{nk_3}+m)\mathrm{F}^{(z)}_{-k_1,n-1}(y)\end{pmatrix}\right], \tag{B9}$$

and

$$\psi^{(-,z)}_{k_1,0,-k_3}(\boldsymbol{r}) = \frac{e^{-ik_1x}e^{-ik_3z}}{2\pi\sqrt{2\omega^{(z)}_{0,k_3}(\omega^{(z)}_{0,k_3}+m)}}C_0\mathrm{F}^{(z)}_{-k_10}(y)\begin{pmatrix}-(1-\lambda)k_3\\ 0\\ \omega^{(z)}_{0,k_3}+m\\ 0\end{pmatrix}, \tag{B10}$$

for $n \geq 1$ and $n = 0$, respectively. The total spatial solution inside the confinement area is given by the linear combination of the left- and right-moving field components as follows:

$$\psi^{(-,z)}_{k_1,n,l}(\boldsymbol{r}) = \psi^{(-,z)}_{k_1,n,k_{3l}}(\boldsymbol{r}) + \psi^{(-,z)}_{k_1,n,-k_{3l}}(\boldsymbol{r}), \tag{B11}$$

where we use $k_{3l}$ to represent the allowed momentum in the system.

## References


[1] H. B. G. Casimir, Kon. Ned. Akad. Wetensch. Proc. **51**, 793 (1948).
[2] M. J. Sparnaay, Physica **24**, 751 (1958).
[3] S. K. Lamoreaux, Phys. Rev. Lett. **78**, 5 (1997); **81**, 5475 (1998) [erratum].
[4] U. Mohideen and A. Roy, Phys. Rev. Lett. **81**, 4549 (1998).
[5] A. Roy, C. Y. Lin, and U. Mohideen, Phys. Rev. D **60**, 111101 (1999).

[6] G. Bressi, G. Carugno, R. Onofrio, and G. Ruoso, Phys. Rev. Lett. **88**, 041804 (2002).
[7] S. Bellucci and A. A. Saharian, Phys. Rev. D **79**, 085019 (2009).
[8] Z. Hassan, S. Ghosh, P. K. Sahoo, and K. Bamba, Eur. Phys. J. C **82**, 1116 (2022).
[9] A. G. Grushin and A. Cortijo, Phys. Rev. Lett. **106**, 020403 (2021).
[10] A. G. Grushin, P. Rodriguez-Lopez, and A. Cortijo, Phys. Rev. B **84**, 045119 (2011).
[11] R. Onofrio, New J. Phys. **8**, 237 (2006).
[12] M. Bordag, U. Mohideen, and V. M. Mostepanenko, Phys. Rept. **353**, 1 (2001).
[13] J. Ambjorn and S. Wolfram, Ann. Phys. **147**, 1 (1983).
[14] A. Chodos, R. L. Jaffe, K. Johnson, C. B. Thorn, and V. F. Weisskopf, Phys. Rev. D **9**, 3471 (1974).
[15] A. Chodos, R. L. Jaffe, K. Johnson, and C. B. Thorn, Phys. Rev. D **10**, 2599 (1974).
[16] K. Johnson, Acta Phys. Polon. B **6**, 865 (1975).
[17] A. Rohim, A. S. Adam, and K. Yamamoto, Prog. Theor. Exp. Phys. **2023**, 013B05 (2023).
[18] C. A. Lutken and F. Ravndal, J. Phys. G **10**, 123 (1984).
[19] Y. A. Sitenko, Phys. Rev. D **91**, 085012 (2015).
[20] M. V. Cougo-Pinto, C. Farina, and A. C. Tort, Conf. Proc. C **9809142**, 235 (1999).
[21] M. Ostrowski, Acta Phys. Polon. B **37**, 1753 (2006).
[22] E. Elizalde, F. C. Santos, and A. C. Tort, J. Phys. A **35**, 7403 (2002).
[23] M. V. Cougo-Pinto, C. Farina, M. R. Negrao, and A. C. Tort, J. Phys. A **32**, 4457 (1999).
[24] C. Farina, Braz. J. Phys. **36**, 1137 (2006).
[25] A. Erdas and K. P. Seltzer, Phys. Rev. D **88**, 105007 (2013).
[26] M. Frank and I. Turan, Phys. Rev. D **74**, 033016 (2006).
[27] A. Martín-Ruiz and C. A. Escobar, Phys. Rev. D **94**, 076010 (2016).
[28] M. B. Cruz, E. R. Bezerra de Mello, and A. Y. Petrov, Phys. Rev. D **96**, 045019 (2017).
[29] A. Erdas, Int. J. Mod. Phys. A **35**, 2050209 (2020).
[30] A. M. Escobar-Ruiz, A. Martín-Ruiz, C. A. Escobar, and R. Linares, Int. J. Mod. Phys. A **36**, 2150168 (2021).
[31] M. Blasone, G. Lambiase, L. Petruzziello, and A. Stabile, Eur. Phys. J. C **78**(11), 976 (2018).
[32] C. A. Escobar, L. Medel, and A. Martín-Ruiz, Phys. Rev. D **101**, 095011 (2020).
[33] M. B. Cruz, E. R. Bezerra de Mello, and A. Y. Petrov, Phys. Rev. D **99**, 085012 (2019).
[34] I. J. Morales Ulion, E. R. Bezerra de Mello, and A. Y. Petrov, Int. J. Mod. Phys. A **30**, 1550220 (2015).
[35] D. R. da Silva, M. B. Cruz, and E. R. Bezerra de Mello, Int. J. Mod. Phys. A **34**, 1950107 (2019).
[36] P. Horava, Phys. Rev. D **79**, 084008 (2009).
[37] V. A. Kostelecky and S. Samuel, Phys. Rev. D **39**, 683 (1989).
[38] D. Colladay and V. A. Kostelecky, Phys. Rev. D **55**, 6760 (1997).
[39] D. Colladay and V. A. Kostelecky, Phys. Rev. D **58**, 116002 (1998).
[40] V. A. Kostelecky, Phys. Rev. D **69**, 105009 (2004).
[41] V. A. Kostelecky and R. Potting, Phys. Rev. D **51**, 3923 (1995).
[42] D. Colladay and V. A. Kostelecky, Phys. Lett. B **344**, 259 (1995).
[43] D. Colladay and V. A. Kostelecky, Phys. Rev. D **52**, 6224 (1995).
[44] B. Schwingenheuer, R. A. Briere, A. R. Barker, L. K. Gibbons, E. Cheu, D. A. Harris, G. Makoff, K. S. McFarland, A. Roodman, Y. W. Wah, et al., Phys. Rev. Lett. **74**, 4376 (1995).
[45] L. K. Gibbons, A. R. Barker, R. A. Briere, G. Makoff, V. Papadimitriou, J. R. Patterson, B. Schwingenheuer, S. V. Somalwar, Y. W. Wah, B. Winstein, et al., Phys. Rev. D **55**, 6625.
[46] R. Carosi, P. Clarke, D. Coward, D. Cundy, N. Doble, L. Gatignon, V. Gibson, P. Grafström, R. Hagelberg, G. Kesseler, et al., Phys. Lett. B **237**, 303 (1990).
[47] V. A. Kostelecky, Phys. Rev. Lett. **80**, 1818 (1998).
[48] P. B. Schwinberg, R. S. Van Dyck, and H. G. Dehmelt, Phys. Lett. A **81**, 2 (1981).
[49] R. S. Van Dyck Jr, P. B. Schwinberg, and H. G. Dehmelt, Phys. Rev. D **34**, 722 (1986).
[50] L. S. Brown and G. Gabrielse, Rev. Mod. Phys. **58**, 233 (1986).
[51] R. S. Van Dyck Jr, P. B. Schwinberg, and H. G. Dehmelt, Phys. Rev. Lett. **59**, 26 (1987).
[52] R. Bluhm, V. A. Kostelecky, and N. Russell, Phys. Rev. Lett. **79**, 1432 (1997).
[53] R. Bluhm, V. A. Kostelecky, and N. Russell, Phys. Rev. D **57**, 3932 (1998).
[54] O. Bertolami, D. Colladay, V. A. Kostelecky, and R. Potting, Phys. Lett. B **395**, 178 (1997).
[55] V. A. Kostelecky and N. Russell, Rev. Mod. Phys. **83**, 11 (2011).

[56] A. Romeo and A. A. Saharian, J. Phys. A **35**, 1297 (2002).
[57] K. Bhattacharya, [arXiv:0705.4275] [Search inSPIRE].
[58] K. Bhattacharya and P. B. Pal, [arXiv:hep-ph/9911498] [Search inSPIRE].
[59] S. M. Carroll and H. Tam, Phys. Rev. D **78**, 044047 (2008).
[60] M. Gomes, J. R. Nascimento, A. Y. Petrov, and A. J. da Silva, Phys. Rev. D **81**, 045018 (2010).
[61] A. Martín-Ruiz and C. A. Escobar, Phys. Rev. D **97**, 095039 (2018).
[62] C. A. Escobar and A. Martín-Ruiz, Phys. Rev. D **99**, 075032 (2019).
[63] A. N. Ivanov, M. Wellenzohn, and H. Abele, Phys. Lett. B **797**, 134819 (2019).
[64] C. A. Escobar, A. Martín-Ruiz, A. M. Escobar-Ruiz, and R. Linares, Eur. Phys. J. Plus **137**, 1186 (2022).
[65] P. Alberto, C. Fiolhais, and V. M. S. Gil, Eur. J. Phys. **17**, 19 (1996).
[66] S. Bellucci and A. A. Saharian, Phys. Rev. D **80**, 105003 (2009).
[67] A. Erdas, Int. J. Mod. Phys. A **36**, 2150155 (2021).